

# Optimal Kalman Filter for state estimation of a quadrotor UAV



Jing-Jing Xiong\*, En-Hui Zheng

College of Mechanical and Electrical Engineering, China Jiliang University, Hangzhou 310018, China

## ARTICLE INFO

*Article history:*  
Received 24 May 2014  
Accepted 3 July 2015

*Keywords:*  
Quadrotor UAV  
State estimation  
Optimal Kalman Filter  
Second order discrete-time sliding mode technique

## ABSTRACT

In this work, the main objective is to study the Optimal Kalman Filtering (OKF) method for estimating the state vector of a small quadrotor UAV through incorporating the internal disturbances including the white Gaussian process and measurement noises. Firstly, the kinematic and dynamic model of the quadrotor is transformed into a discrete-time system via the linear extrapolation method. Secondly, for the sake of performing the high accuracy position and attitude tracking control of the quadrotor, the discrete-time flight controller is designed using second order discrete-time sliding mode technique. In addition, the estimation of the quadrotor aircraft's state vector is carried out with the use of OKF. The performance of the combination between the flight controller and the OKF is evaluated through simulation tests. Extensive simulation results show that the combined strategy has a good performance in terms of variance and state estimation.

© 2015 Elsevier GmbH. All rights reserved.

## 1. Introduction

In recent years, the aerial robotics has been a fast-growing of robotics and multirotor aircraft, especially unmanned aerial vehicles (UAVs), such as the quadrotor (Fig. 1). Low cost and small-size flying platforms are becoming broadly available, and some of these platforms are able to lift relatively high payloads and provide an increasingly broad set of basic functionalities [1]. Quadrotor UAVs already have sufficient payload and flight endurance to support a number of indoor and outdoor applications, and the improvements of battery and other technology are rapidly increasing the scope for commercial opportunities [2]. However, as a necessity for a successful mission, the quadrotor design must be excellent in point of view of the navigation and control system because of the absence of the pilot who can take initiative. The navigation and control system design of the autonomous aircraft is an important topic that is under discussion [3,4].

The necessary state variables of an autonomous quadrotor UAV were estimated via the Kalman Filter (KF) under the condition of sufficient measurements [5]. It is essential that these state variables including position and attitude are accurately obtained to control the aircraft successfully. Meanwhile, both the actuators and sensors should be kept fault free for such an accurate state estimation. Otherwise the KF gives inaccurate results and even derives by time.

Therefore the filter should be built robust in order to achieve fault tolerance in the design of the quadrotor autonomous navigation and control system.

In this work, the Optimal Kalman Filter (OKF) is used to estimate the state variables in the presence of the white Gaussian process and measurement noises, which are caused by the actuator and sensor faults, respectively. The OKF method to the state estimation is quite sensitive to any malfunctions. Moreover, OKF algorithm is adopted here to estimate the state variables from the measurement values of sensors. Considering that the outputs rather than the state variables are obtained by the controller, which holds more substantial reality than [6,7] in which the state variables are utilized by the controller directly.

The results relating to the previously mentioned filter have been given recently in [8–12]. Nowadays, many extended filters based on the standard KF have been developed and applied to the solution of specific problems [4,13–17]. In [13], the extended Kalman Filter (EKF) in its continuous form, the unscented Kalman Filter (UKF) and the spherical simplex unscented Kalman Filter was considered in multibody models. In [4], a robust adaptive Kalman Filter was introduced, which could incorporate measurement and process noise covariance adaptation procedures ( $R$  and  $Q$  adaptation respectively) and utilize adaptive factors in order to adapt itself against sensor/actuator faults. A novel multiple model estimator for the satellite attitude determination system composed of gyroscopes and star sensors was proposed in [14], where the gyroscope drift was obtained from a standard Kalman Filter. A novel quaternion estimator called square-root quaternion cubature Kalman Filter was proposed for spacecraft attitude estimation in [15]. In

\* Corresponding author. Tel.: +86 18072741485.  
E-mail addresses: [jjxiong357@gmail.com](mailto:jjxiong357@gmail.com) (J.-J. Xiong), [ehzheng@cjlu.edu.cn](mailto:ehzheng@cjlu.edu.cn) (E.-H. Zheng).

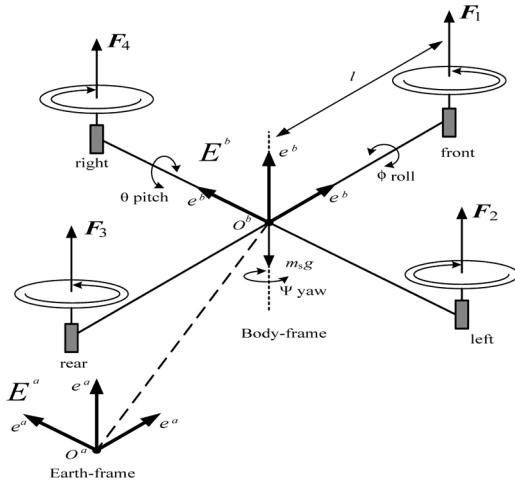


Fig. 1. Quadrotor aircraft.

[16], a resampling ensemble Kalman Filter method was introduced for general nonlinear case. Nonlinear Kalman Filtering and Particle Filtering methods for estimating the state vector of UAVs through the fusion of sensor measurements was studied and compared in [17]. It is noted that all the above papers are not related to the design method of controller and stability analysis of closed-loop system.

In this work, the second order discrete-time sliding mode technique is utilized to design a flight controller for the quadrotor. The remind structure of this paper is organized as follows. In Section 2, the kinematic and dynamic model of the quadrotor is given, and the discrete-time flight controller design is introduced. In Section 3, the OKF for the quadrotor state estimation is illustrated. In Section 4, the simulation tests are performed to evaluate the performance of the combination between the flight controller and the OKF. Section 5 just gives a brief summary of the obtained results and concludes the work.

## 2. Full state feedback control for quadrotor

The kinematic and dynamic model of the quadrotor, shown in Fig. 1, is described in details by Xiong et al. [18,19].

The dynamic characteristics of the quadrotor must be known to build the OKF for the state estimation. In general, six rigid body equations, which consist of three force and three moment equations, are obtained for the quadrotor. According to these papers [18–22], these force and moment equations are written by

$$\begin{cases} \ddot{x} = (\cos \phi \sin \theta \cos \psi + \sin \phi \sin \psi) \frac{u_1}{m} - \frac{K_1 \dot{x}}{m} \\ \ddot{y} = (\cos \phi \sin \theta \sin \psi - \sin \phi \cos \psi) \frac{u_1}{m} - \frac{K_2 \dot{y}}{m} \\ \ddot{z} = (\cos \phi \cos \theta) \frac{u_1}{m} - g - \frac{K_3 \dot{z}}{m} \end{cases} \quad (1)$$

$$\begin{cases} \ddot{\phi} = \dot{\theta} \dot{\psi} \frac{I_y - I_z}{I_x} + \frac{J_r}{I_x} \dot{\theta} \Omega_r + \frac{1}{I_x} u_2 - \frac{K_4 \dot{\phi}}{I_x} \\ \ddot{\theta} = \dot{\phi} \dot{\psi} \frac{I_z - I_x}{I_y} - \frac{J_r}{I_y} \dot{\phi} \Omega_r + \frac{1}{I_y} u_3 - \frac{K_5 \dot{\theta}}{I_y} \\ \ddot{\psi} = \dot{\phi} \dot{\theta} \frac{I_x - I_y}{I_z} + \frac{1}{I_z} u_4 - \frac{K_6 \dot{\psi}}{I_z} \end{cases} \quad (2)$$

where  $x, y$  and  $z$  are the coordinates of the quadrotor center of mass in the inertial frame.  $I_x, I_y$  and  $I_z$  are the moments of inertia among  $x, y$  and  $z$  directions, respectively.  $\phi, \theta$  and  $\psi$  are the roll, pitch and yaw Euler angles.  $K_i$  ( $i = 1, 2, 3, 4, 5, 6$ ) is drag coefficients and positive constants.  $J_r$  is the moment of inertia for each motor.

$\Omega_r = \Omega_1 - \Omega_2 + \Omega_3 - \Omega_4$ ,  $\Omega_i$  ( $i = 1, 2, 3, 4$ ) is the  $i$ th propeller speed,  $\Omega_r$  is the overall speed of propellers.  $m$  is the total mass of the aircraft.  $g$  is the acceleration of gravity.  $l$  is the distance from the center of each rotor to the center of gravity.  $F_i = b\Omega_i^2$  ( $i = 1, 2, 3, 4$ ) is the thrust generated by the  $i$ th rotor.

$$\begin{bmatrix} u_1 \\ u_2 \\ u_3 \\ u_4 \end{bmatrix} = \begin{bmatrix} b & b & b & b \\ 0 & -bl & 0 & bl \\ -bl & 0 & bl & 0 \\ d & -d & d & -d \end{bmatrix} \begin{bmatrix} \Omega_1^2 \\ \Omega_2^2 \\ \Omega_3^2 \\ \Omega_4^2 \end{bmatrix} \quad (3)$$

where  $b$  is thrust coefficient,  $d$  is drag coefficient.

The designed controllers are given as follows [19].

$$\begin{aligned} u_1 &= \frac{m[c_z(\dot{z}_d - \dot{z}) + \ddot{z}_d + g + \varepsilon_1 \text{sgn}(s_1) + \eta_1 s_1] + d_1}{\cos \phi \cos \theta} \\ u_4 &= I_z[c_\psi(\dot{\psi}_d - \dot{\psi}) + \ddot{\psi}_d + \varepsilon_2 \text{sgn}(s_2) + \eta_2 s_2] + d_2 \\ u_3 &= \frac{I_y}{I_c3} \left\{ \begin{aligned} &c_1(\ddot{x}_d - \ddot{x}) + c_2(\dot{x}_d - \dot{x}) + c_3\ddot{\theta}_d \\ &+ c_4(\ddot{\theta}_d - \ddot{\theta}) + \varepsilon_3 \text{sgn}(s_3) + \eta_3 s_3 \end{aligned} \right\} + d_3 \\ u_2 &= \frac{I_x}{I_c7} \left\{ \begin{aligned} &c_5(\ddot{y}_d - \ddot{y}) + c_6(\dot{y}_d - \dot{y}) + c_7\ddot{\phi}_d \\ &+ c_8(\ddot{\phi}_d - \ddot{\phi}) + \varepsilon_4 \text{sgn}(s_4) + \eta_4 s_4 \end{aligned} \right\} + d_4 \end{aligned} \quad (4)$$

where the switching sliding surfaces are

$$\begin{aligned} s_1 &= c_z(z_d - z) + (\dot{z}_d - \dot{z}) \\ s_2 &= c_\psi(\psi_d - \psi) + (\dot{\psi}_d - \dot{\psi}) \\ s_3 &= c_1(\dot{x}_d - \dot{x}) + c_2(x_d - x) + c_3(\dot{\theta}_d - \dot{\theta}) + c_4(\theta_d - \theta) \\ s_4 &= c_5(\dot{y}_d - \dot{y}) + c_6(y_d - y) + c_7(\dot{\phi}_d - \dot{\phi}) + c_8(\phi_d - \phi) \end{aligned}$$

where the state variables with the subscript  $d$  are reference values,  $c_z, c_\psi$  and  $c_i$  ( $i = 1, \dots, 8$ ) are the coefficients of the defined switching sliding surfaces, besides,  $c_z$  and  $c_\psi$  are positive constants,  $c_i$  ( $i = 1, \dots, 8$ ) are obtained by Hurwitz [19],  $d_i$  ( $i = 1, 2, 3, 4$ ) are the disturbances as  $d_1 = K_3 \dot{z}$ ,  $d_2 = -\dot{\phi} \dot{\psi} (I_x - I_y) + K_6 \dot{\psi}$ ,  $d_3 = [-\dot{\phi} \dot{\psi} (I_z - I_x) + J_r \dot{\phi} \Omega_r]$ ,  $d_4 = [-\dot{\theta} \dot{\psi} (I_y - I_x) - J_r \dot{\theta} \Omega_r + K_4 \dot{\phi}] / l$ . The coefficients  $\varepsilon_i$  and  $\eta_i$  ( $i = 1, 2, 3, 4$ ) are positive.

Considering that the force and moment equations of the kinematic and dynamic model of the quadrotor aircraft are the second order equations, and, in order to estimate the state vector for navigation and tracking control, a second order discrete-time system is considered via linear discretization in the following state-space form

$$\begin{aligned} x_1(k+1) &= x_1(k) + x_2(k)T \\ x_2(k+1) &= x_2(k) + f(k)u(k)T + d(k)T \end{aligned} \quad (5)$$

here,  $x_1(k)$  and  $x_2(k)$  are the state variables,  $T$  is a constant sampling period,  $f(k)$  is the coefficient term of the control input,  $u(k)$  is the control input of the system,  $d(k)$  is taken as the disturbance term.

## 3. Optimal Kalman Filter (OKF)

In order to enable navigation of the quadrotor when estimating its state vector by fusing measurements from on-board sensors, the Optimal Kalman Filtering is applied. In the discrete-time case, a linear dynamical system is assumed to be expressed in the form of a discrete-time state model [17,23,24].

$$\begin{aligned} x(k+1) &= Ax(k) + Bu(k) + Gw(k) \\ y(k) &= Cx(k) + v(k) \end{aligned} \quad (6)$$

**Table 1**  
Quadrotor model parameters.

Variables	Values	Units
$m$	2	kg
$l$	0.2	m
$I_x = I_y$	1.2	$N\ s^2/\text{rad}$
$I_z$	2.2	$N\ s^2/\text{rad}$
$J_r$	0.2	$N\ s^2/\text{rad}$
$K_i$ ( $i = 1, 2, 3$ )	0.01	$N\ s/\text{m}$
$K_i$ ( $i = 4, 5, 6$ )	0.012	$N\ s/\text{m}$
$g$	9.8	$\text{m}/\text{s}^2$
$b$	5	$N\ s^2$
$d$	2	$N/\text{ms}^2$

where  $x(k)$  is the state vector at time  $k$ ,  $A$  is the state transition matrix,  $B$  is the control distribution matrix,  $G$  is the transition matrix of system noises,  $y(k)$  is the measurement vector at time  $k$ ,  $C$  is the measurement matrix,  $w(k)$  and  $v(k)$  are the white

**Table 2**  
Controller parameters.

Variables	Values	Variables	Values
$c_z$	1	$c_\psi$	1
$\varepsilon_1$	0.8	$\varepsilon_2$	0.8
$\eta_1$	2	$\eta_2$	2
$c_1$	$11\ \text{m}/(u_1(k)\cos\phi(k)\cos\psi(k))$	$c_5$	$-11\ \text{m}/(u_1(k)\cos\psi(k))$
$c_2$	$6\ \text{m}/(u_1(k)\cos\phi(k)\cos\psi(k))$	$c_6$	$-6\ \text{m}/(u_1(k)\cos\psi(k))$
$c_3$	1	$c_7$	1
$c_4$	6	$c_8$	6
$\varepsilon_3$	0.5	$\varepsilon_4$	0.5
$\eta_3$	5	$\eta_4$	5

Gaussian process and measurement noises with zero means and known covariances.

$$\begin{aligned}
 E[w(k) \cdot w'(j)] &= \begin{cases} Q, & k = j \\ 0, & k \neq j \end{cases}, \\
 E[v(k) \cdot v'(j)] &= \begin{cases} R, & k = j \\ 0, & k \neq j \end{cases}, \\
 E[w(k) \cdot v'(j)] &= 0.
 \end{aligned} \tag{7}$$

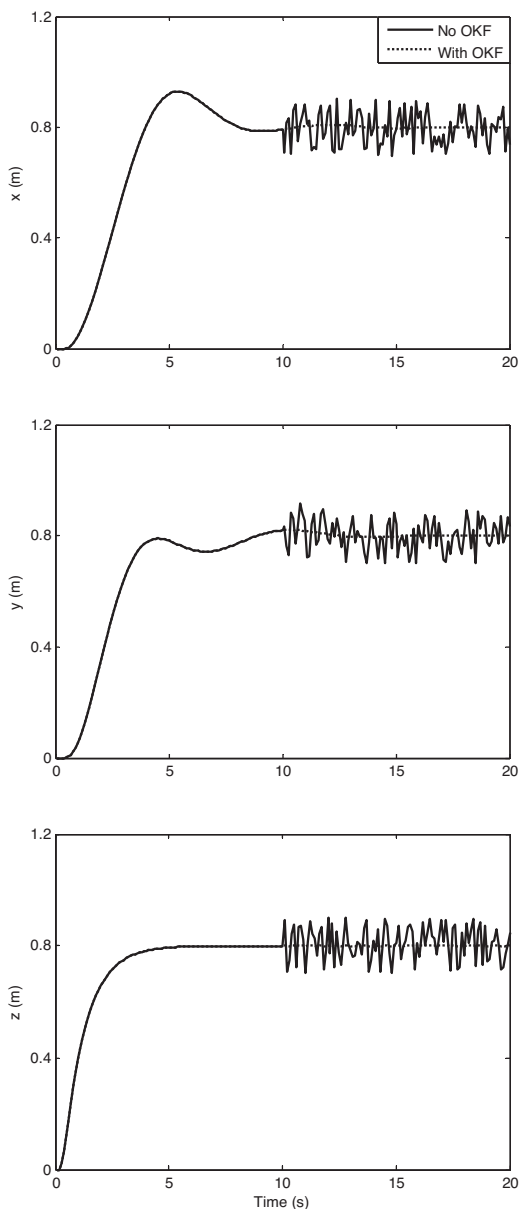


**Fig. 2.** Positions ( $x, y, z$ ), measurement noise.

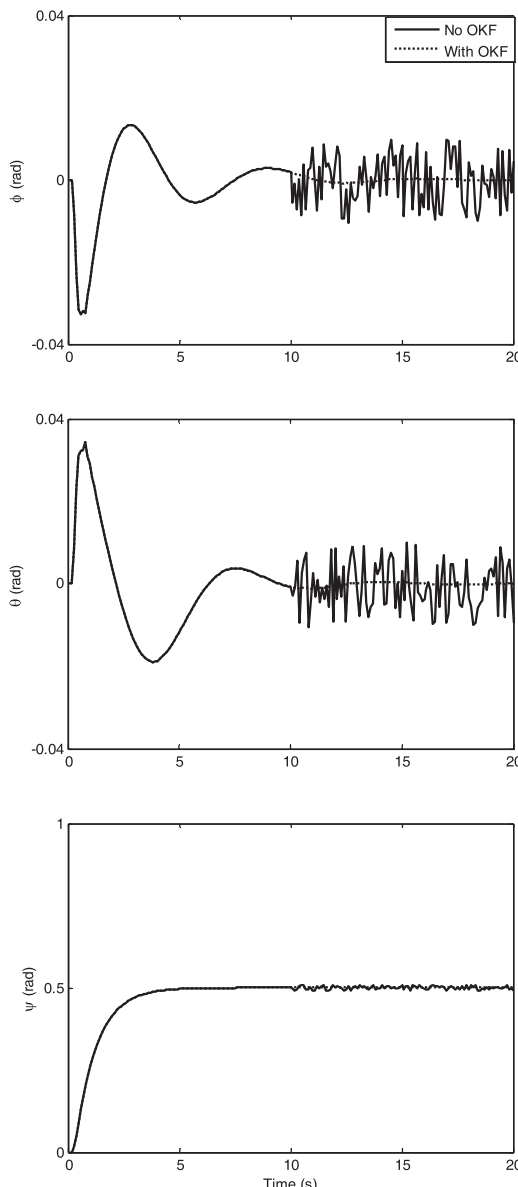


**Fig. 3.** Euler angles ( $\phi, \theta, \psi$ ), measurement noise.

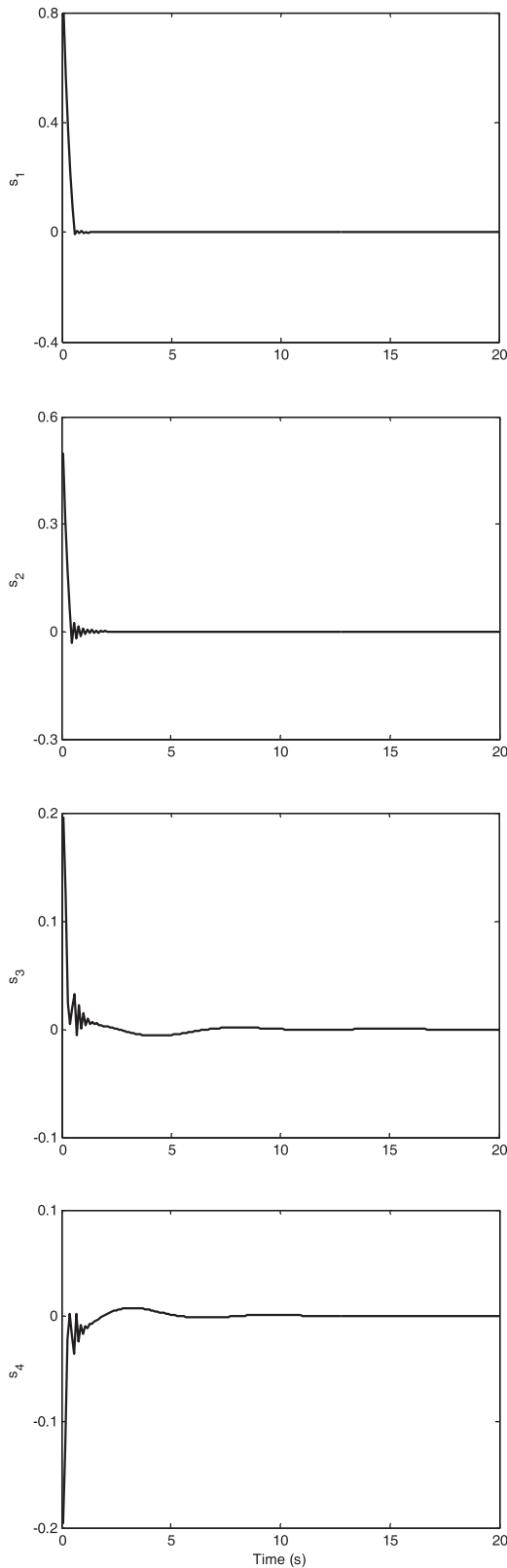


Fig. 4. Sliding variables ( $s_1, s_2, s_3, s_4$ ), measurement noise.

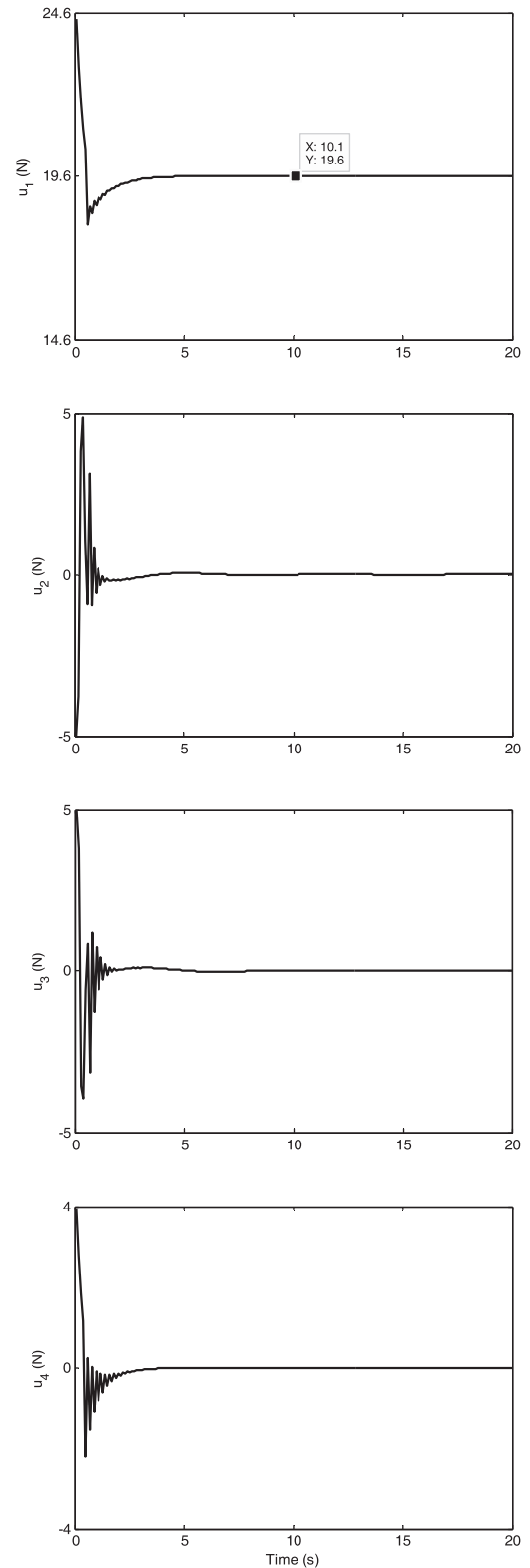


Fig. 5. Flight controllers ( $u_1, u_2, u_3, u_4$ ), measurement noise.

where  $Q$  and  $R$  are known as positive definite matrices.

Hereafter, Optimal Kalman Filter for the combined quadrotor dynamics model is given by the following steps [4]. The initial values of the state vector and the covariance must be given in the derivation process of OKF.

State prediction:

$$x(k | k - 1) = Ax(k - 1 | k - 1) + Bu(k - 1) \tag{8}$$

Covariance prediction:

$$P(k | k - 1) = AP(k - 1 | k - 1)A' + GQG' \tag{9}$$

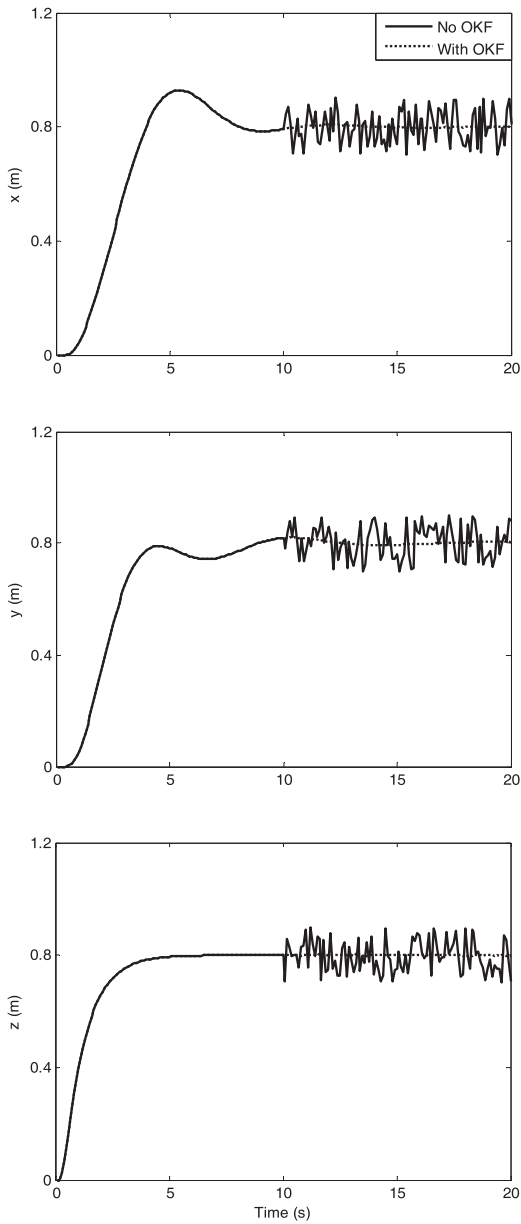


Fig. 6. Positions ( $x, y, z$ ), process and measurement noises.

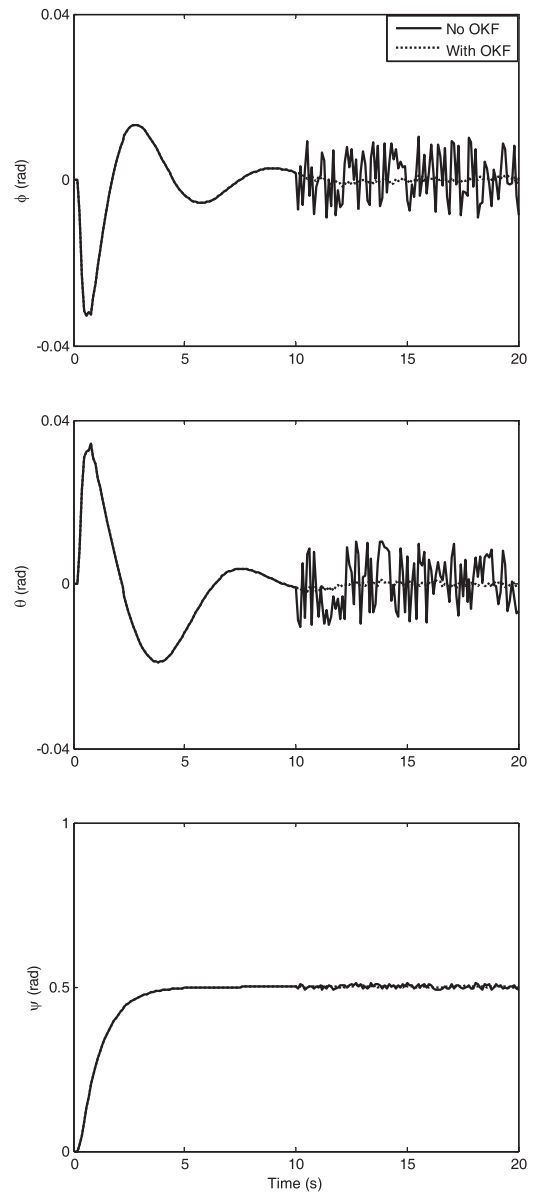


Fig. 7. Euler angles ( $\phi, \theta, \psi$ ), process and measurement noises.

Optimal Kalman gain:

$$N(k) = P(k|k-1)C'(CP(k|k-1)C' + R)^{-1} \tag{10}$$

State estimation:

$$x(k|k) = x(k|k-1) + N(k)(y(k) - Cx(k|k-1)) \tag{11}$$

Covariance estimation:

$$P(k|k) = (I - N(k) \cdot C)P(k|k-1) \tag{12}$$

where Eqs. (8) and (9) predict the filter state vector and corresponding covariance matrix from just after the previous measurement update, or initial condition, respectively, to just before the next measurement. Eq. (10) denotes optimal Kalman gain. Eq. (11) estimates the state vector and Eq. (12) estimates the covariance matrix for discrete step  $k$ .

#### 4. Simulation tests

A model of the quadrotor in Eqs. (1) and (2) is used to test the performances of the combination between OKF and flight controller with respect to the process and measurement noises. In order to perform the high accuracy position and attitude tracking control of the quadrotor, OKF is applied to the control system for estimating the state vector of the quadrotor.

##### 4.1. Measurement noise

In the first test, the assumed Gaussian measurement noise is taken into account the control system. The parameters of OKF include covariances  $Q_i = 1$  and  $R_i = 1$  in Eq. (6), the initial condition  $P_i(0) = 1$  in Eq. (8) ( $i = 1, \dots, 6$ ). The initial conditions of all state variables are  $x(0) = 0, y(0) = 0, z(0) = 0, \phi(0) = 0, \theta(0) = 0, \psi(0) = 0, x(1) = 0, y(1) = 0, z(1) = 0, \phi(1) = 0, \theta(1) = 0, \psi(0) = 0$ .

The reference position and angle values are used in the simulation tests:  $[0.8, 0.8, 0.8]$  m and  $[0,0,0]$  rad. In addition, the quadrotor's model parameters are listed in Table 1 [19], the flight

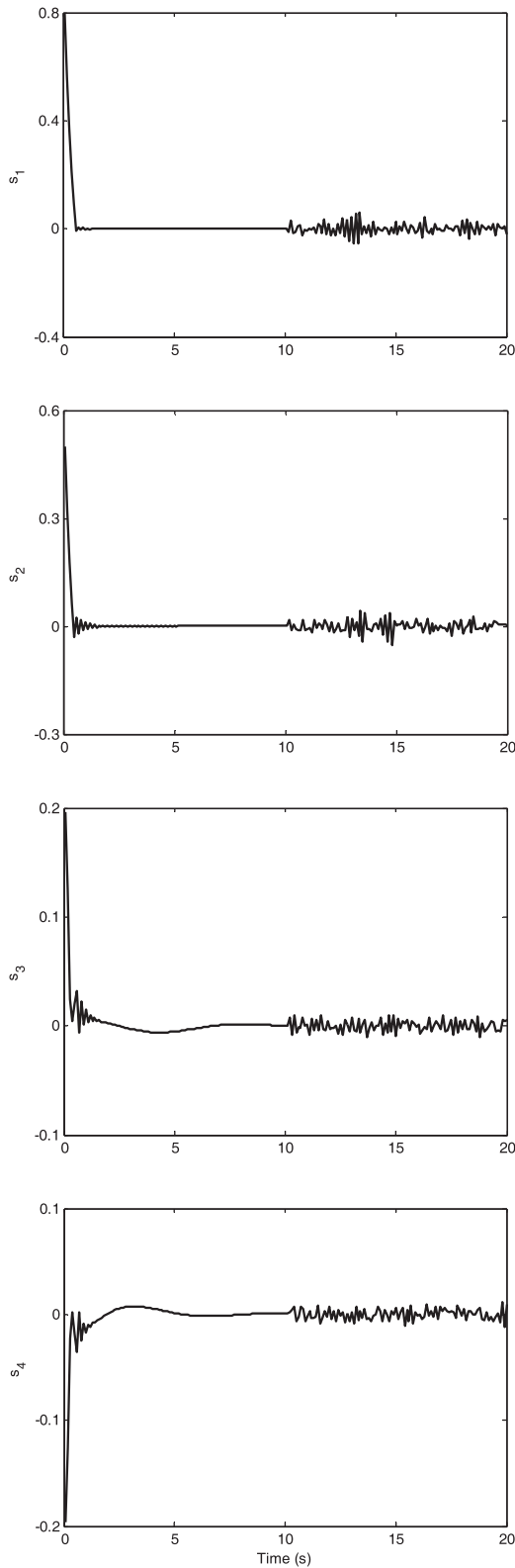


Fig. 8. Sliding variables ( $s_1, s_2, s_3, s_4$ ), process and measurement noises.

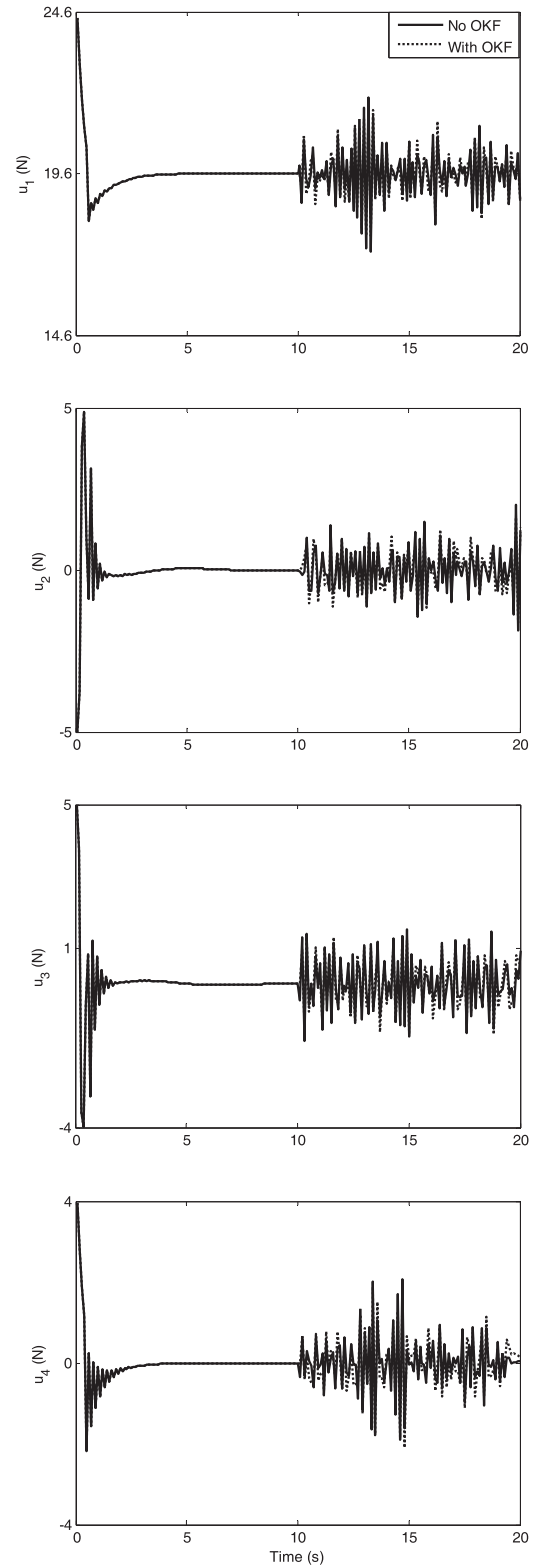


Fig. 9. Flight controllers ( $u_1, u_2, u_3, u_4$ ), process and measurement noises.

controller parameters are listed in Table 2. In addition, the sampling time  $T$  is 0.2 s, the sampled points are 200.

In the simulation performed, the random noises, which are taken as the measurement noise, are added to the six degrees of freedom, and they are applied 10 s after the start of the simulation in the form of random functions, where the positions' amplitudes

are ranged from  $-0.1$  m to  $0.1$  m and the Euler angles' amplitudes are ranged from  $-0.01$  rad to  $0.01$  rad. The simulation results are shown in Figs. 2–5.

From the simulation test presented in Figs. 2 and 3 (which was only performed under the assumption of Gaussian measurement noise), it can be observed that the OKF succeeds good approximation of quadrotor's state vector and subsequently results in good

position and attitude tracking. The number of sample points used by the OKF is so small that it enables fast computation of the quadrotor's state vector.

Simultaneously, it is also shown that even though the quadrotor's state vector are obviously affected by the assumed random noises, OKF is able to estimate and compensate for the state variables quickly, as a result, all the state variables are driven back to the approximate reference state variables. Hereafter, it is demonstrated that OKF has the good performance for estimating state vector with respect to the Gaussian measurement noise.

The behavior of the sliding variables  $s_i$  ( $i = 1, 2, 3, 4$ ), shown in Fig. 4, follows the expectations as all sliding variables converge to their sliding surfaces. Moreover, as desired, the convergence time of  $s_1$  and  $s_2$  is clearly faster than the convergence of  $s_3$  and  $s_4$ . It is noted that, under the OKF and flight controller, the effects of measurement noise are invisible. This, once again, demonstrates the robustness of OKF.

Fig. 5 is a good illustration of the stability of the control system (which was only performed under the assumption of Gaussian measurement noise). The control input variables are approximated to their steady state values with several seconds.

#### 4.2. Process and measurement noises

In this test, the parameters and initial conditions of the quadrotor for simulation are same as the first test. In order to further illustrate the robustness of OKF, the Gaussian process and measurement noises are taken into account the control system. The assumption of measurement noise is applied as the first test, the assumed process noises applied 10 s after the beginning of this simulation in the form of random functions, the amplitudes are ranged from  $-0.5$  to  $0.5$ . The simulation results are shown in Figs. 6–9).

Compared with the test (which was only performed under the assumption of Gaussian measurement noise), the obtained simulation results show that even though the assumed process and measurement noises are applied, and the sliding variables and the flight controller are affected, the high accuracy position and attitude tracking of the quadrotor are not affected. The stability of the quadrotor does not appear affected.

### 5. Conclusions

This work has studied the position and attitude tracking of the quadrotor, when the quadrotor's state vector was estimated by using the assumption of process and measurement noises, respectively. In order to illustrate the robustness with respect to the Gaussian process and measurement noises, the combination between the Optical Kalman Filter and flight controller is performed in MATLAB/Simulink. The main conclusions are summarized as follows. (a) Under the noise disturbances, the high accuracy position and attitude tracking are obtained using the Optical Kalman Filter. (b) The Optical Kalman Filter is an effective estimation method in autonomous navigation systems, especially its good robustness

to measurement noise. (c) The stability of the quadrotor is not affected by the noise disturbances. All above, the presented simulation results are promising at the further exploration of state estimation of the aircraft.

### References

- [1] S. Grzonka, G. Grisetti, W. Burgard, A fully autonomous indoor quadrotor, *IEEE Trans. Robot.* 28 (2012) 90–100.
- [2] B.R. Mahony, V. Kumar, P. Corke, Multirotor aerial vehicles modeling, estimation, and control of quadrotor, *IEEE Robot. Autom. Mag.* 9 (2012) 20–32.
- [3] S.L. Parra, J. Angel, Low cost navigation system for UAVs, *Aerosp. Sci. Technol.* 9 (2005) 504–516.
- [4] C. Hajiyev, H.E. Soken, Robust Adaptive Kalman Filter for estimation of UAV dynamics in the presence of sensor/actuator faults, *Aerosp. Sci. Technol.* 28 (2013) 376–383.
- [5] J. Wendel, O. Meister, C. Schlaile, G.F. Trommer, An integrated GPS/MEMS-IMU navigation system for autonomous helicopter, *Aerosp. Sci. Technol.* 10 (2006) 527–533.
- [6] R.W. Brockett, D. Liberzon, Quantized feedback stabilization of linear systems, *IEEE Trans. Autom. Control* 45 (2000) 1279–1289.
- [7] Y.Q. Xia, J.J. Yan, J.Z. Shang, M.Y. Fu, B. Liu, Stabilization of quantized systems based on Kalman filter, *Control Eng. Pract.* 20 (2012) 954–962.
- [8] Y. Shi, H. Fang, M. Yan, Kalman filter based adaptive control for networked systems with unknown parameters and randomly missing outputs, *Int. J. Robust Nonlinear Control* 19 (2009) 1976–1992 (Special Issue on Control with Limited Information).
- [9] J. Kim, Identification of lateral type force dynamics using an extended Kalman filter from experimental road test data, *Control Eng. Pract.* 17 (2009) 357–367.
- [10] S. Borguet, O. Léonard, Coupling principal component analysis and Kalman filtering algorithms for on-line aircraft engine diagnostics, *Control Eng. Pract.* 17 (2009) 494–502.
- [11] S. Pan, H. Su, J. Chu, W. Hong, Applying a novel extended Kalman filter to missile-target interception with APN guidance law: a benchmark case study, *Control Eng. Pract.* 18 (2010) 159–167.
- [12] M.-F. Hsieh, J. Wang, Design and experimental validation of an extended Kalman filter-based  $\text{NO}_x$  concentration estimator in selective catalytic reduction system applications, *Control Eng. Pract.* 19 (2011) 346–353.
- [13] R. Pastorino, D. Richiedei, J. Cuadrado, A. Trevisani, State estimation using multi-body models and non-linear Kalman filters, *Int. J. Non-linear Mech.* 53 (2013) 83–90.
- [14] K. Xiong, T. Liang, Y.J. Lei, Multiple model Kalman filter for attitude determination of precision pointing spacecraft, *Acta Astronaut.* 68 (2011) 843–852.
- [15] X.J. Tang, Z.B. Liu, J.S. Zhang, Square-root quaternion cubature Kalman filtering for spacecraft attitude estimation, *Acta Astronaut.* 76 (2012) 84–94.
- [16] I. Myrseth, J. Satrom, H. Omre, Resampling the ensemble Kalman filter, *Comput. Geosci.* 55 (2013) 44–53.
- [17] G.G. Rigatos, Nonlinear Kalman Filters and Particle Filters for integrated navigation of unmanned aerial vehicles, *Robot. Auton. Syst.* 60 (2012) 978–996.
- [18] J.-J. Xiong, E.-H. Zheng, Position and attitude tracking control for a quadrotor UAV, *ISA Trans.* 53 (3) (2014) 725–731.
- [19] E.-H. Zheng, J.-J. Xiong, J.-L. Luo, Second order sliding mode control for a quadrotor UAV, *ISA Trans.* (2014), <http://dx.doi.org/10.1016/j.isatra.2014.03.010>
- [20] A. Eresen, N. İmamoğlu, M.Ö. Efe, Autonomous quadrotor flight with vision-based obstacle avoidance in virtual environment, *Expert Syst. Appl.* 39 (2012) 894–905.
- [21] K. Alexis, G. Nikolakopoulos, A. Tzes, Model predictive quadrotor control: attitude, altitude and position experimental studies, *IET Control Theory Appl.* 6 (12) (2012) 1812–1827.
- [22] Y.M. Zhang, et al., Development of advanced FDD and FTC techniques with application to an unmanned quadrotor helicopter testbed, *J. Frankl. Inst.* 350 (2013) 2396–2422.
- [23] G. Rigatos, Q. Zhang, Fuzzy model validation using the local statistical approach, in: 2002 IEEE International Conference on Systems, Man and Cybernetics, 2001, pp. 106–110.
- [24] G.G. Rigatos, *Modelling and Control for Intelligent Industrial Systems: Adaptive Algorithms in Robotics and Industrial Engineering*, Springer, 2011.